



Inland penetration of monsoon depression depends on pre-storm ground wetness – An observational analysis using Self Organizing Maps

Journal:	<i>QJRMS</i>
Manuscript ID:	Draft
Wiley - Manuscript type:	Research Article
Date Submitted by the Author:	
Complete List of Authors:	Kishtawal, Chandra; SAC/ISRO Niyogi, Dev; Purdue University Rajagopalan, Balaji; University of Colorado Mohanty, Uma; Indian Institute of Technology Delhi, Centre for Atmospheric Sciences
Keywords:	indian monsoons, monsoon depressions, soil moisture, self organizing maps, land surface processes



1
2
3
4
5
6 **Inland penetration of monsoon depression depends on pre-storm ground**
7 **wetness – An observational analysis using Self Organizing Maps**
8
9

10 C. M. Kishtawal^{1,2}, Dev Niyogi¹, Balaji Rajagopalan³, M. Rajeevan⁴, N. Jaiswal², and

11
12
13 U.C. Mohanty⁵
14
15

16 1-Purdue University, Department of Agronomy and Department of Earth and Atmospheric
17 Sciences, West Lafayette, IN-47906, USA
18

19
20 2. Space Applications Centre, Indian Space Research Organization, Ahmedabad, India-380015
21

22
23 3-Department of Civil, Environmental and Architectural Engineering, University of Colorado,
24 Boulder, CO-80309, USA.
25

26
27 4. National Atmospheric Research Laboratory, Gadanki, India-517502
28

29
30 5. Indian Institute of Technology-Delhi, New Delhi, India-110016
31
32
33
34
35
36
37
38
39
40
41
42
43
44
45
46
47
48
49
50
51
52
53
54
55
56
57
58
59
60

Abstract

Using the tracks of 183 monsoon depressions (MDs) formed in the Bay of Bengal during 1951 and 2004 and the gridded analysis of daily rainfall fields for the same period, we assessed the association between length of post-landfall inland penetration by monsoon depressions and the pre-storm rainfall. Pre-storm rainfall is treated as a surrogate to pre-storm ground wetness conditions due to unavailability of historical soil-moisture data over the monsoon region. These observations were analyzed using Self Organizing Maps (SOM) to discretize the pre-storm rainfall. The SOM approach revealed nine different prototypes that characterize the pre-storm monsoon rainfall patterns into different transition states like active, active-to-break, break-to-active, break etc. Analysis of MDs linked to each prototype shows that MD's with higher inland penetration were associated with higher pre-storm rainfall, in other terms, under higher ground wetness conditions. On the other hand, the genesis of a large number of MDs was associated with dry pre-storm conditions over the land, while the MDs associated with this state could travel significantly smaller distance after their landfall. (Case study of one representative MD generated and developed under anomalous dry land conditions suggests that the positioning of tropical convergence zone (TCZ) over the Bay of Bengal could be attributed both to the genesis of higher number of MDs as well as the dry inland condition prior to the formation of MDs). Higher number of MD genesis were found to be associated with following pre-existing conditions (a) consistency of tropical convergence zone as indicated by rainfall patterns, and (b) larger gradients of sea-level pressure over the northern Bay of Bengal. The main conclusion that appears from the present study is that pre-storm ground wetness conditions favorably affect the inland penetration length of monsoon depressions that also implies the larger lifespan of these storms over the land.

1.0 Introduction

Monsoon depressions (MDs hereinafter) are probably the most important rain bearing weather systems for Indian subcontinent that occur during the Indian summer monsoon (ISM) season. Using the ECMWF model reanalysis fields, Yoon and Chen (2005) reported that MDs contribute to about 45-55% of total monsoon seasonal rainfall, and that their rainfall structure is largely maintained by convergence of atmospheric water vapor flux coupled with the lower tropospheric divergent circulation. The unique topography of Indian peninsula and Indo-china/Myanmar region favors the formation and development of monsoon depressions in the warm and moist air over the Bay of Bengal (Holt and Sethuraman, 1986). After their formation the MDs move in a north-northwest track along the monsoon trough to the warmer and drier heat low regions of Northwest India and Pakistan. Goswami (1987) concluded that the west-northwest movement of the MDs is due to the generation of Rossby-gravity waves to the west of the initial diabatic heat source over the Bay of Bengal that creates maximum moisture convergence in the WNW direction, leading to a continuous positive feedback loop and the observed movement of MDs. Latent heat release due to organized convection (Shukla, 1978) and barotropic instability (Krishnamurti et al., 1980, Nitta and Masuda, 1981) have been shown to be important mechanisms for the development of MDs. The genesis of MDs in the head of the Bay of Bengal is believed to be linked to the location of monsoon trough in relation to the Gangetic plains (Holt and Raman, 1986). About 4-5 monsoon depressions form in each monsoon season providing copious amount of rainfall along their tracks (Krishnamurti 1979, Sikka, 1977).

Due to the significance of the MDs in the ISM rainfall, the length of their inland penetration and the amount time spent by MDs over the land are the topics of major concern. Tropical

1
2
3 systems weaken rapidly after landfall due to the lack of surface moisture fluxes (Kaplan and
4 DeMaria 1995). Heterogeneities in the landscape structure (e.g., in soil moisture, surface
5 roughness, albedo, vegetated land cover, stomatal conductance, etc.) tend to create mesoscale
6 boundaries that can impact mesoscale circulation, convection and precipitation (Anthes, 1984,
7 Avissar and Liu, 1996, Segal 1992, Pielke 2001, Pielke and Niyogi 2009). Soil moisture plays a
8 predominant role because of its key influence on the partitioning of energy into sensible and
9 latent heat fluxes at the ground surface (Alapaty et al. 1997). Dastoor and Krishnamurti (1991)
10 reviewed the role of soil wetness on a Bay of Bengal MD using a mesoscale numerical weather
11 prediction model and suggested that the extremely dry land surface would stall the storm motion,
12 while a extremely wet land surface would weaken the storm, as well as produce weaker but more
13 widespread precipitation. In their study, the improved ground wetness parameterization resulted
14 in simulated rainfall closer to observation over coastal and inland regions in the Indian monsoon
15 region. Recently in Chang et al. (2009) we developed a process based assessment of three
16 landfalling MDs and concluded that wetter antecedent land surface can intensify the landfalling
17 MDs over the Indian monsoon region.

18
19
20
21
22
23
24
25
26
27
28
29
30
31
32
33
34
35
36
37
38
39
40 The present study mainly focuses on the association of inland penetration of MDs with pre-
41 storm wetness conditions. Due to unavailability of historical records of soil moisture over the
42 monsoon region, we used the pre-storm rainfall as a surrogate to the ground wetness conditions.
43
44
45
46
47
48
49
50
51
52
53
54
55
56
57
58
59
60
The underlying hypothesis that we aim to test through the present analysis is that pre-storm
ground wetness favorably affects the post-landfall behavior (e.g. lifespan and intensity) of
monsoon depressions.

2.0 Data and methods

We investigate the relation between prestorm surface wetness (surrogated by prestorm rainfall) and inland penetration by discretizing the pre-storm rainfall into countable number of states using the the Kohonen's Self Organizing Map (SOM) (Kohonen 1988; Kohonen 1990; Hewitson and Crane 2002) and then by determining the association of MDs inland penetration length (IPL) with these patterns. Details regarding the MD observations and the analysis are presented here.

2.1 Tracks of MDs: Monsoon depression tracks were obtained from the recently compiled electronic atlas of tropical cyclones and monsoon depressions by IMD (IMD e-atlas, 2007). The atlas contains the tracks for several MDs over the period 1891-2007. The region of the genesis of MDs in the Bay of Bengal is in vicinity of the land mass and the quality of historical MD location data (e.g. latitude/longitude positions) is considered good owing to the existence of a meteorological observational network in colonial India since as early as 1857. For the present study we considered only those MDs that formed in the Bay of Bengal between June and September (or the summer monsoon season) during the period 1951-2004, for which, gridded observations of surface rainfall were also available. Fig. 1 shows the tracks of all the MDs that formed over the Bay of Bengal during the monsoon seasons (June-September) between the years 1951 and 2004. For the period 1951-2004 (coincident with the rainfall observations), tracks for 189 such MDs were available, and 183 MDs actually crossed the landmass over the Indian subcontinent. These 183 cases were considered for further analysis. The inland penetration by these MDs varies from 30 km to 2350 km.

1
2
3 2.2 *Rainfall data*: Daily gridded rainfall data at 1° grid spacing from India Meteorological
4 Department (IMD) [Rajeevan *et al.*, 2006] were used. This dataset is based on 2140 stations over
5 India with a minimum 90% data availability during the period 1951-2004. Using these station
6 data, the grid-point analysis of rainfall was prepared using the Shepard's directional interpolation
7 method [Shepard, 1968] over the Indian subcontinent (6.5° N to 37.5° N, 66.5°E to 101.5° E).
8 Standard quality controls were performed before carrying out the interpolation analysis. Due to
9 averaging, the gridded rainfall data are smoother compared to individual station data.
10
11
12
13
14
15
16
17
18
19

20 2.3 Kohonen Self Organizing Maps

21 We used the “Self Organized Maps” (SOM) for characterizing the pre-storm rainfall into
22 patterns that can be used in interpretation of the physical processes linking them to the observed
23 behavior of MDs. SOM methods represent the class of “unsupervised classification”, and uses
24 the technique of machine-learning in an artificial neural network (ANN) framework. SOMs have
25 been used earlier for the identification of atmospheric precursors to extreme rainfall (Cavazos,
26 1999), analysis of preferred states of monsoon intraseasonal oscillations (Sahai and
27 Chattopadhyay, 2006, SC-06 hereafter), and analysis of synoptic climatic patterns (Hewitson and
28 Crane, 2002).
29
30
31
32
33
34
35
36
37
38
39
40
41
42

43 The basic objective of SOM in most of the climatic applications is to group the events (that are
44 represented by 2-D or even 3-D fields of some atmospheric parameter, like 2D-rainfall fields in
45 the present case) into separate classes according to some similarity criteria (SC-06). The number
46 of classes, or, clusters, onto which the input fields are to be mapped, are called the “nodes” of
47 SOM, and are generally represented in the form of a 2-dimensional grid. The SOM can be used
48 to partition the input data to smaller regions by associating input data with their best-matching
49
50
51
52
53
54
55
56
57
58
59
60

units from higher dimensions onto a two dimensional grid of lattice points (Kohonen, 1990). Each data point in input space has, by definition, one best matching unit. The aim of Self-Organization is to generate a topology preserving mapping, where the neighborhood relations in the input space are preserved as well as possible, in the neighborhood relations of the units of the map (Lampinen and Oja,1989). The SOM algorithm works in the following manner. Let $\mathbf{X} = [x_1, x_2, \dots, x_n]^T \in \mathbb{R}^n$ be the input vector of real numbers. Assume a discrete lattice of units indexed with a index i . Each node contains the corresponding weight vector $\mathbf{W}_i = [w_{i1}, w_{i2}, \dots, w_{in}]^T \in \mathbb{R}^n$. \mathbf{X} is mapped to the unit whose weight vector is its nearest neighbor, from among all the weight vectors. This is called the best matching unit and is found by using

$$|\mathbf{X} - \mathbf{W}_j| = \min_i |\mathbf{X} - \mathbf{W}_i| \quad (1)$$

One important step in this procedure is to select the number of nodes of SOM. There is little guidance in the literature about the optimum number of nodes for SOMs. A rule of thumb used by many investigators in cluster analysis is $C_{\max} < \sqrt{n}$ where C_{\max} is the maximum number of clusters and n denotes the number of observations. Jian and Quiansheng (2001) demonstrated the validity of this rule through a detailed theoretical analysis. For our sample size of for $n=183$, the SOM nodes should be less than (4X4), and hence we used a (3X3) square topology to train the SOM. Results from a symmetric topology like square are easy to interpret. The training procedure for the SOM is completely objective and data adaptive. The SOM nodes are initialized with random weight vectors with a strict condition that no two nodes have identical weights (SC-06). Input data vectors are broadcasted parallel to all the neurons and for each input vector the most responsive neuron is located. The weight vector associated with this neuron and predefined

neighborhood neurons, which are assigned randomly initially, are adjusted to reduce the Euclidean distance with the input vector. The training utilizes competitive learning. When a training example is fed to the network, its Euclidean distance to all weight vectors is computed (Haykin, 1999). The neuron with weight vector most similar to the input is called the best matching unit (BMU). The weights of the BMU and neurons close to it in the SOM lattice are adjusted towards the input vector. The magnitude of the change decreases with time and with distance from the BMU. The update formula for a neuron with weight vector $\mathbf{W}(t)$ is

$$\mathbf{W}(t + 1) = \mathbf{W}(t) + \Theta(v, t) \alpha(t)(\mathbf{D}(t) - \mathbf{W}(t)) \quad (2)$$

where $\alpha(t)$ is a monotonically decreasing learning coefficient and $\mathbf{D}(t)$ is the input vector at a given iterative time step 't'. The neighborhood function $\Theta(v, t)$ depends on the lattice distance between the BMU and neuron v . In the simplest form it is one for all neurons close enough to BMU and zero for others, but a gaussian function is a common choice, too. Regardless of the functional form, the neighborhood function shrinks with time.

The main objective of using SOM in the present study is to group the rainfall conditions before the formation of MDs into a small number of clusters, where each cluster is represented by some SOM node. The SOM algorithm acts such that distance between two nodes on SOM map is indirectly proportional to the similarity between the patterns (input vectors) projected on those nodes. Thus at the end of SOM training phase, one gets a set of unique patterns representing possible distinct states that the input vector had assumed within the given data set.

After deciding what represents "pre-storm rainfall"(taken as a measure of the antecedent soil wetness), we collected the mean fields of pre-storm rainfall for all 183 MDs. These are 2-D fields of mean gridded rainfall. These 183 rainfall fields are then subjected to SOM analysis. Thus the only feature common among these rainfall fields is that they belong to a period just

1
2
3 prior to the formation of some MD. SOM analysis clusters these fields on the basis of the
4 similarity of “rainfall” in terms of distribution and intensity, and not on the basis of the nature of
5
6 MDs that follow these rainfall events. The analysis of MDs corresponding to different classes of
7
8 rainfall patterns obtained after SOM analysis is carried out in the next step.
9
10
11

12 13 14 15 **4.0 Results**

16 17 **4.1 Nature of MDs**

18 19 20 21 22 *(a) Intraseasonal variability*

23
24
25
26
27 We used a longer record of MD observations (1901-2007) just for the analysis of their general
28 behavior. A total number of 434 MDs formed over the Bay of Bengal during the monsoon season
29 for the period 1901-2007. The MDs propagate predominantly towards the northwest direction
30 along a narrow corridor that nearly coincides with the seasonal monsoon trough. 15% of the total
31 MDs were formed in the month of June, 25% in July, 35% in August, and 25% in September
32 (Fig. 2-a). After crossing the coastline, the MDs were found to travel to western side as far as
33 66°E and to northern side as far as 33°N before dissipation. Monsoon depressions show a
34 pronounced intraseasonal variability both in terms of the genesis and post-landfall life span. MD
35 activity begins with the onset of the summer monsoon season around second week of June and
36 lasts till the end of September (Fig. 2). After the second week of July, MD activity shows a
37 significant increase, and MD activity is generally high till second week of September. The peak
38 in the “number of MD occurrences” occurs in the last week of July, while the maximum inland-
39 penetration occurs during late-August and early September. The intraseasonal variability of ISO
40
41
42
43
44
45
46
47
48
49
50
51
52
53
54
55
56
57
58
59
60

shows a skewed pattern with a larger number of MDs and their larger inland penetration occurring during the second half of monsoon season. There is larger asymmetry in the distribution of inland penetration compared to the number of formations. This asymmetric pattern itself is indicative of the link between pre-storm ground wetness and the inland-behavior of MDs. Even though the monsoon season begins from the first week of June, it progresses slowly towards north (Webster et al., 1998), and by first week of July, the monsoon covers the entire Indian subcontinent. Due to this reason, the land-surface is expected to be wetter during the second half of the monsoon season.

(b) Probability distribution of Inland Penetration Length

The range of the inland penetration length (computed by measuring the length of the track after landfall) varied from 30 km to 2350 km with 90% of MDs dissipating before travelling 1450 km inland. Fig. 3 shows the probability density function (PDFs) of IPL for MDs. The representation of the PDFs in analytical form is helpful for interpretation, analysis and simulation of events. The PDF can be expressed as a simple two-parameter Weibull distribution of the following form:

$$f(x) = \frac{\alpha}{\beta} \left(\frac{x}{\beta}\right)^{\alpha-1} \exp\left(-\left(\frac{x}{\beta}\right)^{\alpha}\right) \quad (3)$$

Where $\alpha = 1.1961$ is the continuous shape parameter, and $\beta = 730.1357$ is the continuous scaling parameter. The goodness-of-fit can be tested both qualitatively, by visual comparison of the data with the distribution, and also quantitatively. The quantitative test most often used is the Lillefors test, a variation on the Kolmogorov-Smirnov test used for testing the fit of a distribution

1
2
3 when the test is being conducted using the same data that were used to fit the distribution (Wilks,
4 2006). This test compares the D_n test statistic (the largest difference, in absolute value, between
5
6 the empirical and fitted cumulative distribution functions) with a critical value determined by the
7
8 number of observations in the dataset and the chosen significance level (Wilks, 2006).
9
10 Qualitative fit-tests used often include simple plots of the data histogram with the fitted
11
12 distribution overlaid, and Quantile-Quantile ('Q-Q') plots and Percentile-Percentile (P-P) plots.
13
14 P-P plots show the values of the theoretical cumulative distribution function (CDF) compared
15
16 with the observed CDF. This gives a summary of how well the fitted distribution represents the
17
18 data across the whole distribution. A good fit will closely follow the line $x=y$. The Weibull
19
20 distribution was also tested for the goodness of fit using Kolmogorov Smirnov entropy test ,
21
22 Anderson-Darling test, and Chi-square test, and was found to be acceptable by all the above. Fig.
23
24 4-a shows the modeled distribution. Both P-P , and Q-Q plots (figure not shown) indicate that the
25
26 Weibull distribution is the most suitable representation of the probability of inland penetration of
27
28 MDs.
29
30
31
32
33
34
35
36
37
38
39
40

41 *(c) Long term variation of monsoon depressions*

42
43 Fig. 4 shows the long term variation of occurrence and inland penetration of monsoon
44
45 depressions for the period 1891-2007. Both the inland penetration length and number of MDs
46
47 per season show multi-decadal scale variations, with no appreciable trends (Fig 4 a,b). Fig. 4-
48
49 a shows that the period between 1920 and 1950 was the most active phase in terms of the
50
51 genesis of MDs. There was a consistent reduction of MD occurrences between 1950 and
52
53 2000, but there were indications of the revival of MD activity during the recent decade, with
54
55
56
57
58
59
60

1
2
3 the formation of above average number of MDs during the years 2006 (6 MDs) and 2007 (5
4 MDs) and close to average number of MDs during 2008(4 MDs). This finding contrasts the
5
6 notion expressed by other researchers that there is a decreasing trend in the frequency of
7
8 occurrence of monsoon depressions (Dash et al, 2000) and appears to be because of the
9
10 different period of records. Similarly, the inland penetration seems to have a decreasing trend
11
12 during the first three decades of the past century. However, the dominant component of long-
13
14 term variability is still appears multi-decadal in nature. It is interesting to note from the
15
16 available data that the long-term cyclic behavior of the number of MDs and their inland
17
18 penetration are in opposite phase. In other words, epochs with higher number of MD
19
20 formations are also the epochs with smaller inland penetration. Forthcoming analysis of the
21
22 present study also suggests that a larger number MDs with shorter inland penetration are
23
24 associated with pre-existing dry land conditions. This inverse phase relationship between the
25
26 number and the length of inland penetration suggests that the total energy associated with
27
28 monsoon transient systems like MDs is generally conserved at least at the epochal time scale.
29
30 How the interplay among planetary and monsoon scale circulation and the land-atmosphere
31
32 interaction maintains the stability of the monsoon rainfall (Niyogi et al., 2009) is intriguing
33
34 as well as interesting and deserves a detailed theoretical investigation.
35
36
37
38
39
40
41
42
43
44

45
46 *(d) SOM of pre-storm rainfall*
47

48 The first step towards generation of SOM is the preparation of input vector that is the pre-storm
49 mean rainfall in the present study. In a recently published study, Chang et al. (2009) indicated a
50 link between pre-storm rainfall and the inland-lifespan of MDs. A simple correlation analysis
51 suggests that the pre-storm rainfall along the land-corridor of MDs (or monsoon trough region,
52
53
54
55
56
57
58
59
60

1
2
3 indicated by the area tracked by majority of MDs in Fig. 1) is relevant for the post-landfall life-
4 span of MDs. In order to determine the most suitable indicator of pre-storm rainfall, we averaged
5 the rainfall over the monsoon corridor for a period (T_0-N) days to (T_0-N-M) days, where T_0 is the
6 date of MD formation reported by IMD, N indicates the “lag” (i.e. the time before the MD
7 formation), and M the period for averaging. The average rainfall was then correlated to IPL for
8 different values of N and M . Fig.-5a shows the correlation of IPL with pre-storm rainfall over the
9 monsoon trough region for various lags (1-15 days) and averaging windows (1-15 days, going
10 backward from the day of the lag). Results indicate that the IPL is best correlated with the pre-
11 storm rainfall averaged for the period (T_0-1) day to (T_0-7) days where T_0 is the reported date of
12 MD formation in the Bay of Bengal. Thus for each of the 183 MDs, we selected 7-day mean
13 antecedent rainfall over 190 grid-points (of $1^\circ \times 1^\circ$ size) along the monsoon trough, Fig-5b shows
14 the mean pre-storm rainfall averaged for 183 MDs. This antecedent rainfall formed our basic
15 input vector for further processing.
16
17
18
19
20
21
22
23
24
25
26
27
28
29
30
31
32
33

34 Fig. 6 shows the results of SOM analysis, which yielded nine different states of pre-storm
35 rainfall over India. These nine states are projected onto a 3X3 matrix shown in Table 1. The table
36 also shows the number of MDs, mean prestorm rainfall and mean IPL represented by each SOM
37 node. The SOM patterns (Fig. 6) indicate a gradual and systematic transition of rainfall from one
38 state to another. Node [3,1] shows the typical situation of a well developed “active” state of the
39 monsoon with tropical convergence zone (TCZ, indicated by rainfall distribution) located over
40 core monsoon region. In this mode, rain-rates typically exceed 20 mm/day, and relatively dry
41 situations prevail to the north and to the south of TCZ. The diagonally opposite node [1,3]
42 indicates a dry pre-storm land conditions that may occur during the early phase of monsoon
43 during June, periodic monsoon “breaks”, and during the withdrawal of monsoon after the second
44
45
46
47
48
49
50
51
52
53
54
55
56
57
58
59
60

1
2
3 half of September. Rain rates during this phase seldom exceed 3 mm/day. Two nodes adjacent
4 to [1,3] i.e. nodes [1,2] and [2,3] also denote dry situations over core monsoon region and also
5
6 over NW India, but also represent relatively wetter condition on north-eastern and southern sides
7
8 respectively. These two nodes indicate the culmination and termination of monsoon break
9
10 periods. Node [1,1] shows the transition of “active” to “break” monsoon situation when TCZ
11
12 migrates northward and lies along the foothills of the Himalayas (Sikka and Gadgil, 1980), while
13
14 node [3,3] denotes the “break-to-active” transition with TCZ at south-peninsular India and dry
15
16 situation to the north. Other nodes indicate the “normal” situations of monsoon with wide-
17
18 spread rainfall extending from south-east to northwest parts of India.
19
20
21
22
23
24
25
26

27 The correlations between the IPL and pre-storm rainfall rates averaged for each node is 0.826
28
29 indicating a clear link between antecedent surface wetness and post-landfall lifespan of
30
31 monsoon depressions. Another interesting pattern that emerges from this analysis is that the
32
33 largest number of MD events are associated with the four corners of SOM, e.g. nodes
34
35 [1,1],[1,3],[3,1], and [3,3]. These four nodes account for 70% of the land falling MDs. . The
36
37 SOM classification procedure ensures that the nodes at extreme corners represent the largest
38
39 dissimilarities among the corresponding patterns. The four corner nodes in Fig. 6 denote
40
41 different stages of summer monsoon intraseasonal variability. One feature common to these
42
43 extreme nodes is the alignment of the orientation of rain bands (in case of nodes [1,1],[3,1], and
44
45 [3.3]) or the dryness (in case of node [1,3]) with the monsoon trough axis. Also, in case of wet
46
47 nodes (e.g. association with high rainfall activity over the land), the pre-storm rainfall is
48
49 concentrated over a well defined narrow region, indicating the stability of TCZ during a week-
50
51 long period before the formation of MDs. It is possible that the factors such as the stability of the
52
53
54
55
56
57
58
59
60

1
2
3 low level convergence associated with TCZ, its favorable positioning along the monsoon trough
4 and over the northern region of the Bay of Bengal, and the warm and moist conditions of the Bay
5 of Bengal together make the conditions favorable for the mesoscale eddies to intensify to become
6 monsoon depressions. In case of prolonged monsoon breaks, represented by node [1,3], the
7 radiative heating quickly warms the land surface. If the extent and duration of dryness and
8 warming is sufficiently large, a shallow heat-low can form over the Indian subcontinent
9 (Ramage, 1971, Raghavan, 1973) that typically extends from arid north-west region to the Bay
10 of Bengal coast along the monsoon trough axis. The dryness over the Indian subcontinent could
11 also be a result of the compensating subsidence associated with the TCZ positioned over the Bay
12 of Bengal and Indo-China region.
13
14
15
16
17
18
19
20
21
22
23
24
25
26

27 Fig. 7 shows the distribution of inland penetration by MDs represented by each SOM node. Each
28 vertical bar in this figure represents one MD event, while the length of the bar denotes the inland
29 penetration length by that MD. The largest number of MD formations are found to be associated
30 with dry pre-storm conditions (node [1,3]) and a lesser number of formations were associated
31 with pre-storm conditions where pre-storm rainfall was concentrated over narrow trough zones
32 (nodes [1,1],[3,1],and [3,3]). _The association of dry land conditions over NW-India and the
33 formation of MDs is clearly highlighted by node [1,3] which denotes extreme dry situation over
34 NW-India. This SOM node alone is associated with highest number of 48 MD formations in the
35 Bay of Bengal during the period of study. However, these MDs do not seem to survive longer
36 after crossing the land due to inadequate supply of water vapor flux. The average IPL for MDs
37 belonging to this node is 490 km, while only 25% of those could travel beyond 600 km. A large
38 fraction of MD formations coincide with “active” and “active-to-break transition” phases of
39 monsoon compared to “break-to-active transition” states, which can be attributed to the
40
41
42
43
44
45
46
47
48
49
50
51
52
53
54
55
56
57
58
59
60

1
2
3 favorable positioning of the eastern part of monsoon trough over the warm and moist regions of
4 the Bay of Bengal. During the active and active-to-break phase the tail of monsoon trough lies
5 over the northern portion of the head of Bay of Bengal, where sea surface temperature and
6 orography are more favorable to the formation of MD. The mean rainfall for all the MD cases on
7 each node was highly correlated to the average IPL for that node ($r=0.83$), although only 9 pairs
8 of averages were used for the correlation.
9

10 We analyzed two MDs – one each from two extreme pre-storm rainfall patterns viz SOM node
11 [3,1] denoting very dry conditions before the formation of MD, and node [1,3] denoting active
12 monsoon conditions. The first MD corresponding to node [3,1], or dry pre-storm conditions,
13 formed in the Bay of Bengal on 5 August 1972, and slowly moved inland in west-northwest
14 direction, and finally got dissipated on 11 August 1972. In its lifespan of 7 days, MD-1 travelled
15 a distance of 1200 km, making it one of the slowest moving MDs. The other monsoon
16 depression, MD-2, formed in the head of the Bay of Bengal on 4-Aug-1997, and moved in west-
17 northwest direction, a little south to the track of MD-1, and terminated in northwest India on 7-
18 Aug-1997. During the four day period of its life, MD-2 covered an inland distance of about 1750
19 km, and was one of the fastest moving monsoon depressions. Using the NCEP/NCAR reanalysis,
20 the pre-storm atmospheric conditions and their possible role in the later development and
21 movement of these monsoon depressions were analyzed.
22
23
24
25
26
27
28
29
30
31
32
33
34
35
36
37
38
39
40
41
42
43
44
45
46
47

48 The pre-storm land conditions for MD-1 (SOM node [1,3]) were extremely dry and
49 corresponded to the “monsoon break” situation. Fig. 9(a, b) shows the patterns of SLP and
50 precipitation averaged for the period 29-Jul-1972 to 4-Aug-1972, denoting the pre-storm period.
51
52
53 With dry conditions prevailing over the land, the SLP patterns denote a “heat-trough” (Figure not
54
55
56
57
58
59
60

1
2
3 shown), normally associated with shallow convergence and upward motion at the lower layers
4
5 (surface-850 hPa) and divergence and sinking motion above 850 hPa (Blake et al., 1983). The
6
7 heat-trough axis trails at the head of the Bay of Bengal. During the same period, the TCZ seen as
8
9 the axis of maximum cloudiness (Sikka and Gadgil, 1980, Yasunari 1981), is situated along a
10
11 southwest to northeast axis, and coincides with the eastern part of heat trough over the head of
12
13 the Bay of Bengal. Unlike heat trough, the TCZ is associated with a deep and strong convergence
14
15 from surface to 400 hPa (Asnani 1993) and associated downdrafts on both sides of TCZ. It is
16
17 possible that the dry conditions and downward atmospheric motion over India at this period are
18
19 linked to the positioning of TCZ over the Bay of Bengal and the strong and deep convergence
20
21 associated with it. This is evident from Fig. 8-b, which shows the average vertical velocity
22
23 (omega) at 850 hPa during 28-July-to-03-Aug-1972. This figure shows large scale sinking
24
25 motion (positive omega) over the Indian subcontinent and an upward motion over the Bay of
26
27 Bengal, prior to the formation of MD. In fact we observed the same pattern of vertical velocity
28
29 for several other MDs linked to the dry SOM node, and the location of TCZ, along with the
30
31 associated downward motion over India which explains to some extent the cause of pre-storm
32
33 dryness for this node as well as a large number of MD genesis linked to it. Chen et al (2005)
34
35 denoted that the sources of diabatic heating (e.g. precipitation) on the west-southwest side of a
36
37 MD are conducive for its maintenance and growth. Thus we see that atmospheric conditions like
38
39 (i) the presence of "heat-trough" over the land trailing over the Bay of Bengal, and (ii) the
40
41 presence of strong TCZ, along with the availability of diabatic energy sources at the southern
42
43 portion, were favorable to the growth of an instability like MD. Whether TCZ alone was
44
45 sufficient to support the genesis and the growth of the MD, or the continental heat trough also
46
47
48
49
50
51
52
53
54
55
56
57
58
59
60

1
2
3 played a role in the initiation of this instability, is not clear, and certainly deserves further
4
5 analysis.
6
7

8 The genesis of second monsoon depression, MD-2 [4-7 Aug, 1997], was concurrent with the
9
10 active monsoon conditions over the Indian subcontinent, with TCZ passing through the center of
11
12 India, and trailing at the Bay of Bengal. During the active phase of monsoon, the “heat-trough”
13
14 is replaced by the TCZ, with significantly stronger and deeper convergence. The cyclonic
15
16 vorticity associated with TCZ is much more structured and enhanced which can be inferred from
17
18 the patterns of pre-storm stream function fields computed from the average circulation during the
19
20 period 28-Jul-to-03-Aug, 1997 (Fig. not shown). Interestingly the westward gradients of pre-
21
22 existing stream function fields are well-defined, structured and negatively stronger than those
23
24 associated with MD-1. Pre-existing rainfall over the Indian peninsula and a larger spread of
25
26 upward vertical velocity (Fig. 8-c,d) helped the MD2 to grow rapidly and penetrate deeper into
27
28 the land.
29
30
31
32
33
34
35

36 In an interesting study, Singh et al. (2004) found that more monsoon depressions form in
37
38 the Bay of Bengal when the Indian subcontinent experienced poor monsoon conditions e.g.
39
40 during the El Niño years.. Whether dry conditions over the land is a cause or an effect of larger
41
42 number of MD formations in the Bay of Bengal is not clear and can be a subject of detailed
43
44 investigation in future studies. Chen et al. (2005) proposed a mechanism for the westward
45
46 propagation of MDs due to the negative streamfunction tendency west of the depression center
47
48 caused by the vortex stretching created by the upward branch of the east–west asymmetric
49
50 circulation across the depression. This upward branch of a MDs east–west circulation coupled
51
52 with a divergent circulation is maintained by the latent heat released by cumulus convection/
53
54
55
56
57
58
59
60

1
2
3 rainfall over the depression's west-south-west sector. The convection/rainfall is then maintained
4
5 by the convergence of water vapor flux driven by the lower-tropospheric divergent circulation.
6
7 Our results also indicate that the supply of water vapor flux, from the wet surface conditions,
8
9 would be important for the westward propagation of MDs.
10
11

12
13 The active and break cycle of monsoon system can be viewed as the periodic northward
14
15 transition of the TCZ from the north equatorial Indian Ocean to the foothill of Himalayas
16
17 (Sikka and Gadgil, 1980). During the active phase, TCZ lies over the core monsoon region,
18
19 extending from NW-India to the Bay of Bengal. The complex interaction between the high
20
21 cyclonic vorticity associated with the monsoon trough and the orography on the northern and
22
23 eastern sides of the Bay of Bengal can deform the lower tropospheric circulation to make it
24
25 barotropically unstable for the growth of mesoscale circulation patterns such as the MDs. The
26
27 genesis of the MDs can also be viewed as the "splitting" of the large cyclonic eddy, e.g. the
28
29 large scale monsoon flow around the trough due to orographically induced shearing deformation.
30
31 MDs generated during the active phase of monsoon are supported by the ground wetness due to
32
33 pre-storm rainfall, which is evident from the larger in-land penetration by MDs belonging to
34
35 node [3,1].
36
37
38
39
40
41
42

43
44 The occurrence of a large number of MDs during significant dry conditions over the land,
45
46 (particularly over the NW India) is intriguing, and the mechanism is probably linked to the same
47
48 factors that cause the onset of the monsoon, and at times, the transition of monsoon from break
49
50 to active state. The major transition between wet and dry monsoon states is the replacement of
51
52 TCZ with heat-trough circulation, due to rapid increase of surface temperature under dry
53
54 monsoon conditions. Heat-trough circulation dominates the early phase of the monsoon and is
55
56
57
58
59
60

1
2
3 one of the critical triggers for the seasonal reversal of low level monsoon circulation (Ramage,
4 1971). Yasunari (2007) suggested that the highest atmospheric sensitivity to the land-surface
5 forcings (such as surface wetness anomalies) can be found over the dry and semi-arid regions of
6 monsoon e.g. the NW India. Our results hint that the rapid modifications of low-pressure over
7 the NW India under dry conditions could favor the formation of MDs in the Bay of Bengal, and
8 needs to be answered through analytical and modeling studies. Goswami et al(2003) carried out
9 the analysis of clustering of synoptic activity (like MDs and low pressure systems), and
10 concluded that the active monsoon situation is more conducive for the genesis of such synoptic
11 events. While Goswami et al(2003) used a broad classification of monsoon activity as “active”
12 and “break”, the SOM analysis in the present study delineated the patterns of monsoon activity at
13 finer scale, focusing more on the transition states of monsoon activity. In the broad sense, our
14 analysis does not contrast the findings of Goswami et al(2003), as a large number of MD
15 formations indeed belong to active phase of monsoon, represented by top and right side panels of
16 Fig. 6. However, our analysis indicates that among the various “transition” states of monsoon
17 activity, the “break” situation contributes to the largest share of the formations of MDs.
18
19
20
21
22
23
24
25
26
27
28
29
30
31
32
33
34
35
36
37
38
39
40
41
42

43
44 *(e) Patterns of pre-storm sea level pressure*

45 We analyzed the patterns of mean sea level pressure (SLP) two days prior to the formation of
46 each of the MDs projected on different SOM nodes, using the daily averaged analysis from
47 NCEP-NCAR reanalysis data (Kalnay et al. 1996). Fig. 9 shows the mean pre-storm SLP
48 anomaly fields (termed as pre-SLP hereafter), averaged for corresponding number of events for
49 each SOM node. Anomalies are computed by subtracting the pre-storm SLP averaged for all 183
50
51
52
53
54
55
56
57
58
59
60

1
2
3 storms from that for individual storms, while the term “pre-storm” refers to the 7 day period
4
5 between (T_0-1) day to (T_0-7) days. One of the common characteristic features of pre-SLP
6
7 patterns is a prominent trough extending from NW-India to the Bay of Bengal. The sharp
8
9 curvature of SLP contours in the northern Bay of Bengal produces ideal low level atmospheric
10
11 circulation that is conducive for the growth of mesoscale eddies into MDs. Strong east-west
12
13 gradients of pre-SLPs are coincident with the positive rainfall activity over Indian subcontinent
14
15 which indicates the presence of TCZ over the land extending up to the Bay of Bengal. On the
16
17 other hand, the dry node [1,3] is associated with weaker east-west pressure gradients. Despite
18
19 the general similarity of pre-SLP patterns there are noticeable differences in the strength, and
20
21 spatial gradients of pre-SLP patterns from one node to another. For at least four nodes, the traces
22
23 of remnant low pressure systems can be seen as weak and closed isobar over the Indo-China sea.
24
25 Saha et al. (1981) showed that the origin of about 60% of the MDs can be traced back to the
26
27 westward moving low pressure systems at the Thailand and Myanmar coasts which intensify
28
29 over the Bay of Bengal under the favorable conditions. It is interesting to note that pre-SLP
30
31 patterns for nodes [1,1], [1,3], and [3,1], that were associated with about half of the MD
32
33 occurrences, did not show prominent low pressure remnants at the eastern side, indicating that
34
35 these MDs originated over the Bay of Bengal. Large pre-SLP gradients for nodes [1,1] and [3,1]
36
37 can be strong enough to induce the barotropic instability for the local genesis of MDs. To
38
39 analyze the differences in pre-SLP patterns for the different MDs, we computed the pre-SLP
40
41 anomaly for each node with respect to the average pre-SLP for all 183 MDs. The anomaly fields
42
43 bring out interesting link between the number of MD formations and the gradients of pre-SLP
44
45 anomaly over the northern Bay of Bengal. For all the nodes with large number of MD
46
47 formations, there was a large gradient of pre-SLP over the northern Bay of Bengal, although
48
49
50
51
52
53
54
55
56
57
58
59
60

1
2
3 there is no consistent pattern in the nature of the gradient. Nodes [1,1] (26 MDs) and [3,3] (28
4 MDs) show larger zonal anomaly of pre-SLP, while nodes [1,3] (48 MDs), [3,1](26 MDs), and
5 [3,2](15 MDs) show meridional anomaly at the head of the Bay of Bengal. Interestingly, the dry
6 node [1,3] associated with highest number of 48 MDs, shows largest meridional gradients of pre-
7 SLP in the North Bay of Bengal which is also the location of the genesis of most of the MDs.
8 Conversely, the nodes with least MD formations , e.g. [2,1] (7 MDs), [2,2] (8 MDs), and [2,3]
9 (10 MDs) show weakest gradients of pre-SLP over the head Bay. From the viewpoint of
10 geostrophic balance of the winds, both south-to-north and east-to-west gradients of SLP should
11 eventually lead to the generation of cyclonic vorticity, and this partially explains the link
12 between the number of MD formations and the anomaly of the pre-SLP fields.
13
14
15
16
17
18
19
20
21
22
23
24
25
26
27
28
29
30
31

32 **Conclusions**

33
34 Using the tracks of 183 monsoon depressions (MDs) formed in the Bay of Bengal during 1951
35 and 2004 and the gridded analysis of daily rainfall fields for the same period we explored the
36 association between the pre-storm rainfall and the length of post-landfall inland penetration by
37 monsoon depressions. The technique of Self Organizing Maps (SOM) was used to discretize the
38 pre-storm rainfall and nine prototypes were obtained. These prototypes showed that in general,
39 the larger inland penetration by MDs is associated with higher pre-storm rainfall amounts. The 7
40 day period between T_0-1 days to T_0-7 days (T_0 being the reported date of the formation of MDs)
41 shows the maximum and statistically significant correlation with the penetration length, and this
42 is considered the optimum estimate of the pre-storm rainfall amount. There is significantly larger
43 number of MD formations over the head of the Bay of Bengal during “active” and “active-to-
44
45
46
47
48
49
50
51
52
53
54
55
56
57
58
59
60

1
2
3 break” transition states of monsoon compared to “break-to-active” transition. Interestingly, the
4
5 largest number of MD formations were associated with very dry pre-storm conditions. This dry
6
7 mode is identified to represent the early (early June), late (late September) or the break phase of
8
9 the monsoon. The analysis of one typical MD associated with this dry mode suggests that the
10
11 favorable positioning of TCZ over the head of the Bay of Bengal, with or without the interaction
12
13 with continental heat trough may create conducive situations for the growth of these instabilities.
14
15 Positioning of TCZ over the Bay of Bengal/ Indo-China region may also be contributing to the
16
17 dryness over Indian subcontinent due to compensating subsidence of dry and warm air
18
19 associated with strong convergence along the TCZ.. Larger inland penetration of MDs for wetter
20
21 pre-storm conditions supports the view of earlier researchers (Dastoor and Krishnamurti, 1991,
22
23 Yoon et al., 2005, Chang et al. 2009) that a regular supply of lower tropospheric water vapor is
24
25 essential for the maintenance of the structure of an MD. On the other hand, the genesis of a large
26
27 number of MDs was associated with dry pre-storm conditions over the land, while these MDs
28
29 could travel significantly smaller distance after their landfall. Patterns of pre-storm stream
30
31 function fields suggest a weak westward gradient of cyclonic vorticity for dry land condition and
32
33 a stronger gradient for wetter condition. Although Chen et al (2005) showed the generation of
34
35 negative tendency of stream function west of MDs as the mechanism for the westward
36
37 propagation of MDs., some of the present analysis suggests that the westward and negatively
38
39 strong gradients of pre-storm stream function fields may also be linked to the westward
40
41 propagation of MDs.
42
43
44
45
46
47
48
49

50
51 **Acknowledgements:** Study benefited in part from NSF CAREER-0847472 (Liming Zhou and
52
53 Jay Fein) and NASA Terrestrial Hydrology Program (Jared Entin).
54
55
56
57
58
59
60

References

Alapaty, K., S. Raman, and D. S. Niyogi, 1997: Uncertainty in specification of surface characteristics: A study of prediction errors in the boundary layer. *Bound.-Layer Meteor.*, **82**, 473–500.

Anthes R.A., 1984: Enhancement of convective precipitation by mesoscale variations in vegetative covering in semiarid regions. *Jour. Clim. Appl. Meteorol.*, **23**:865-889.

Asnani G C, 1993 : *Tropical Meteorology Vol. 1*, Indian Inst. Trop. Meteorol., Pune, 603 pp.

Avissar R, and Y. Liu, 1996: Three-dimensional numerical study of shallow convective clouds and precipitation induced by land surface forcing. *Journal of Geophysical Research*. **101(D3)**:7499-518.

Blake, D W, T N Krishnamurti, S V Low-Nam and J S Fein, 1983: Heat low over the Saudi Arabian desert during May 1979 (summer MONEX), *Mon. Weather. Rev.*, **111**, 1759-1775.

Cavazos, T., 1999, Large scale circulation anomalies conducive to extreme precipitation events and derivation of daily rainfall in northern eastern Mexico and southeastern Texas, *J. Climate*, **12**, 1506-1523, 1999.

Chang H., D. Niyogi, A. Kumar, C. Kishtawal, J. Dudhia, F. Chen, U.C. Mohanty, M. Sheperd, 2009,

Chen T.C., J.H. Yoon, and S.Y. Wang, 2005 : Westward propagation of the Indian monsoon depression. *Tellus*, **57A**, 758-769.

Dash S.K., Jenamani Rajendra Kumar, and M.S. Shekhar, 2004: On the decreasing frequency of monsoon depressions over the Indian region. *Current Science*, **86**, 1404-1411.

Dastoor A., and T.N. Krishnamurti, 1991: The landfall and structure of a tropical cyclone : The sensitivity of model predictions to soil moisture parameterizations. *Boundary Layer Meteorol.*, **55**, 345-380.

Goswami B.N., 1987 : A mechanism for the west-north-west movement of monsoon depressions.

1
2
3 Goswami, B N, R.S Ajaya Mohan, Prince K Xavier and D. Sengupta, 2003:Clustering of Low
4 Pressure Systems During the Indian Summer Monsoon by Intraseasonal Oscillations, *Geophys.*
5 *Res. Lett.* 30 (8), 1431, doi: 10.1029/ 2002GL016734, 2003.
6
7

8
9
10 Haykin, S., 1999: "Self-organizing maps". *Neural networks - A comprehensive foundation* (2nd
11 edition ed.). Prentice-Hall. ISBN 0-13-908385-5.
12

13
14 Hewitson, B C , and R G Crane, 2002: Self organizing maps: application to synoptic
15 climatology. *Climate research*.22:13-26.
16

17
18
19 Holt T., and Sethu Raman, 1986 : A comparison of the significant features of the marine
20 boundary layers over the Arabian Sea and the Bay of Bengal during MONEX-79. Proc. Of
21 National Conference on FGGE, Jan. 14-17, 1986.
22

23
24
25 Jian Y U, and Quinsheng C, 2001 : The upper bound of the optimal number of clusters in fuzzy
26 clustering. *Science in China* , 44, 119-125.
27

28
29
30 Kalnay, E., and co-authors (1996), The NCEP/NCAR 40-Year Reanalysis Project, *Bull. Amer.*
31 *Meteorol. Soc.*: 77, 437–472.
32

33
34
35 Kaplan, J., and M. DeMaria, 1995: A simple empirical model for predicting the decay of tropical
36 cyclone winds after landfall. *J.Appl. Meteor.*, 34, 2499–2512.
37

38
39 Kohonen, T., 1990 : The self organizing map. *Proc IEEE* .78(9):1464-1480.
40

41
42 Kohonen T., 1988:. *Self-Organization and Associative Memory*, volume 8 of Series in
43 Information Sciences. Springer-Verlag, 2nd edition, 1988.
44

45
46
47 Krishnamurti T.N., Y. Ramanathan, P. Ardanuy, R. Pasch and P. Grieman, 1980 : Quick look
48 summer MONEX atlas. Pt-III Monsoon Depression phase. Rep. 80-8, FSU, 135 pp.
49

50
51 Krishnamurti, T.-N. 1979. Tropical Meteorology. In: *Compendium of Meteorology II* (ed.
52 A.Wiin-Nielsen), WMO-No. 364,World Meteorological Organization, 428 pp.
53
54
55
56
57
58
59
60

1
2
3 Lampinen J., and E.Oja. Fast self-organization by the probing algorithm. In Proceedings of the
4 International Joint Conference on Neural Networks, IJCNN, pages II 503 – II 507, 1989.

5
6
7
8 *Nature* **326**, 376 - 378 (26 March 1987); doi:10.1038/326376a0

9
10 Nitta T., and K. Masuda, 1981 : Observational study of a monsoon depression developed over
11 the Bay of Bengal during summer MONEX. *J. Meteor. Soc. Japan*, 59, 672-682.

12
13
14
15 Niyogi, D., C.M. Kishtawal, S. Tripathi, R. S. Govindaraju, 2009, Observational Evidence that
16 agricultural Intensification and land use change may be reducing the Indian Summer Monsoon
17 Rainfall, *Water Resources Research*, in press

18
19
20
21 Pielke, Sr. R. A. 2001: Influence of the spatial distribution of vegetation and soils on the
22 prediction of cumulus convective rainfall. *Rev. Geophys.* , 39, 151-177.

23
24
25
26 Pielke Sr. R A, and D Niyogi, 2009: The role of landscape processes within the climate system.
27 In: Otto, J.C. and R. Dikaum, Eds., *Landform - Structure, Evolution, Process Control:*
28 *Proceedings of the International Symposium on Landforms organised by the Research Training*
29 *Group 437. Lecture Notes in Earth Sciences, Springer, Vol. 115, in press.*

30
31
32
33 Possible relation between land surface feedback and the post-landfall structure of monsoon
34 depression, *Geophys. Res. Ltr.* , 36, L15826, doi:10.1029/2009GL037781

35
36
37
38 Raghavan, K., 1973, Break monsoon over India, *Mon. Wea. Rev.*, 101, 33 – 43.

39
40
41
42 Rajeevan, M., J. Bhate, J.D. Kale, and B. Lal , 2006: High resolution daily gridded rainfall data
43 for Indian region: Analysis of break and active monsoon spells, *Current Science*, 91, 3, 296-306.

44
45
46 Ramage, C. S., *Monsoon Meteorology*. Academic Press, New York and London, 296 pp., 1971.

47
48
49 Saha, K., Sanders, F. and Shukla, J. 1981. Westward propagating predecessors of monsoon
50 depressions. *Mon. Wea. Rev.* 109, 330–343.

1
2
3 Sahai, A K, and Chattopadhyay, 2006 : An objective study of Indian summer monsoon
4 variability using the self organizing map algorithm. IITM Research Report RR-113, 41-pp.
5 (Available from Indian Institute of Tropical Meteorology, Pune, India-411008)
6
7

8
9
10 Segal M, and R.W. Arritt, 1992 : Nonclassical mesoscale circulations caused by surface sensible
11 heat-flux gradients. Bulletin of American Meteorological Society 1992;73:1593-604.
12

13
14 Shepard, D, 1965 : A two-dimensional interpolation function for irregularly spaced data. Proc.
15 23rd Nat. Conf. ACM, p-517.
16

17
18 Shukla J., 1978 : CISK barotropic instability and the growth of monsoon depressions. J. Atmos.
19 Sci., 35, 495-508.
20

21
22 Sikka, D and S Gadgil, 1980 : On the maximum cloud zone and the ITCZ over Indian longitudes
23 during the southwest monsoon. Mon Weather Rev. 108, 1840-1853.
24

25
26 Sikka, D. R. 1977. Some aspects of the life history, structure and movement of monsoon
27 depressions. *Pure Appl. Geophys.* 115, 1501–1529.
28

29
30 Singh O.P., T.M.A. Khan, and M.Z. Rahman, 2004 : Impact of Southern Oscillation on the
31 Frequency of Monsoon Depressions in the Bay of Bengal. *Natural Hazards*, 25,2,101-115.
32

33
34 Taylor CM, Said F, Lebel T, 1997:. Interactions between the land surface and mesoscale rainfall
35 variability during HAPEX-Sahel. *Monthly Weather Review*. 125(9):2211-2227.
36

37
38 Webster P.J., V. O. Magafia, T. N. Palmer, J. Shukla, R. A. Tomas, M. Yanai, and T.
39 Yasunari, 1998 : Monsoons: Processes, predictability, and the prospects for prediction. *J.*
40 *Geophys. Res.*, **103**, 14,451-14,510.
41

42
43 Wilks, D, 2006: Statistical methods in the atmospheric sciences (second edition), Elsevier,
44 Oxford, 2006.
45

46
47 Yasunari T., 2007 : Role of land-atmosphere interaction on Asian monsoon climate. *Jou. Met.*
48 *Soc. Japan*, 85-B, 55-75.
49
50
51
52

1
2
3 Yasunari, T., 1981 : Structure of the Indian monsoon system with around 40--day period, 59, J.
4 Meteorol. Soc. Jpn, 225—229.
5
6

7
8 Yoon, J-H. and Chen, T.-C., 2005. Water vapor budget of the Indian monsoon depression. *Tellus*
9 57A, 770–782.
10
11
12
13
14
15
16
17
18
19
20
21
22
23
24
25
26
27
28
29
30
31
32
33
34
35
36
37
38
39
40
41
42
43
44
45
46
47
48
49
50
51
52
53
54
55
56
57
58
59
60

For Peer Review

Table-1 : Summary of SOM analysis of pre-storm rainfall for 183 monsoon depressions.

[1,1] 7.52 <u>795 km</u> N=26	[2,1] 9.18 <u>950 km</u> N=7	[3,1] 10.45 <u>754 km</u> N=26
[1,2] 5.11 <u>595 km</u> N=15	[2,2] 7.15 <u>779 km</u> N=8	[3,2] 9.51 <u>846 km</u> N=15
[1,3] 3.62 <u>494 km</u> N=48	[2,3] 5.75 <u>647 km</u> N=10	[3,3] 8.52 <u>715 km</u> N=28

(Entries in each cell are in the following order (i) Numbers within square brackets denote the index of SOM node (ii) mean pre-storm rainfall rate for all MDs projected on a node (iii) mean inland penetration by MDs (iv) number of MDs projected on a node)

Figures Captions

1. Tracks of all the monsoon depressions originating from the Bay of Bengal during monsoon season (1951-2004)
2. Intraseasonal variation of MDs (a) Average monthly occurrences of MDs (b) Average monthly inland penetration by MDs (c) total number of MDs formed on each day monsoon season during the period 1891-2007 (dashed line shows unfiltered values, solid line shows smoothed values) (d) same as Fig. 4-c, but for the mean inland penetration (Km) by MDs..
3. PDF of inland penetration length by MDs and the fitted Weibull distribution.
4. (a) Long term variation of number of MDs per year (1891-2007) and (b) mean penetration length by MDs (Km). (Dashed lines show unfiltered values while solid lines show smoothed values)
5. (a) Correlation of IPL with pre-storm rain for various lags and averaging periods (b) mean pre-storm rainfall (for lag = 1 day and averaging period = 7 days) for all 183 cases.
6. Patterns of pre-storm rainfall projected on SOM nodes. (The order of different nodes in this figure is as indicated in Table-1.)
7. Inland penetration lengths by MDs for different SOM nodes. Each vertical bar denotes one MD event while the length of the bar represents the inland penetration. (The order of different nodes is as indicated in Table-1)
8. Sample figure showing the 7-day average patterns of (a) vertical velocity (ω) and (b) rainfall before the formation of an MD [formation date : 05-Aug-1972] during dry phase (SOM node [1,3]). (c), and (d) show the same parameters as (a) and (b) respectively, but for an MD during the wet node [3,1]. The later MD formed on 04-Aug-1997.
9. Average patterns of pre-storm sea level pressure (SLP-minus 1000 hPa) for MDs projected on different SOM nodes. The index of each node as shown in Table-1. The

1
2
3 negative values are shaded. SLP fields denote the situation 2 days prior to the formation
4 of MDs.
5
6

7
8 10. Same as Fig. 9 but for SLP anomalies (unit=Pascal). Anomalies are computed with
9 respect to the average pre-storm SLP for all 183 MDs.
10
11
12
13
14
15
16
17
18
19
20
21
22
23
24
25
26
27
28
29
30
31
32
33
34
35
36
37
38
39
40
41
42
43
44
45
46
47
48
49
50
51
52
53
54
55
56
57
58
59
60

For Peer Review

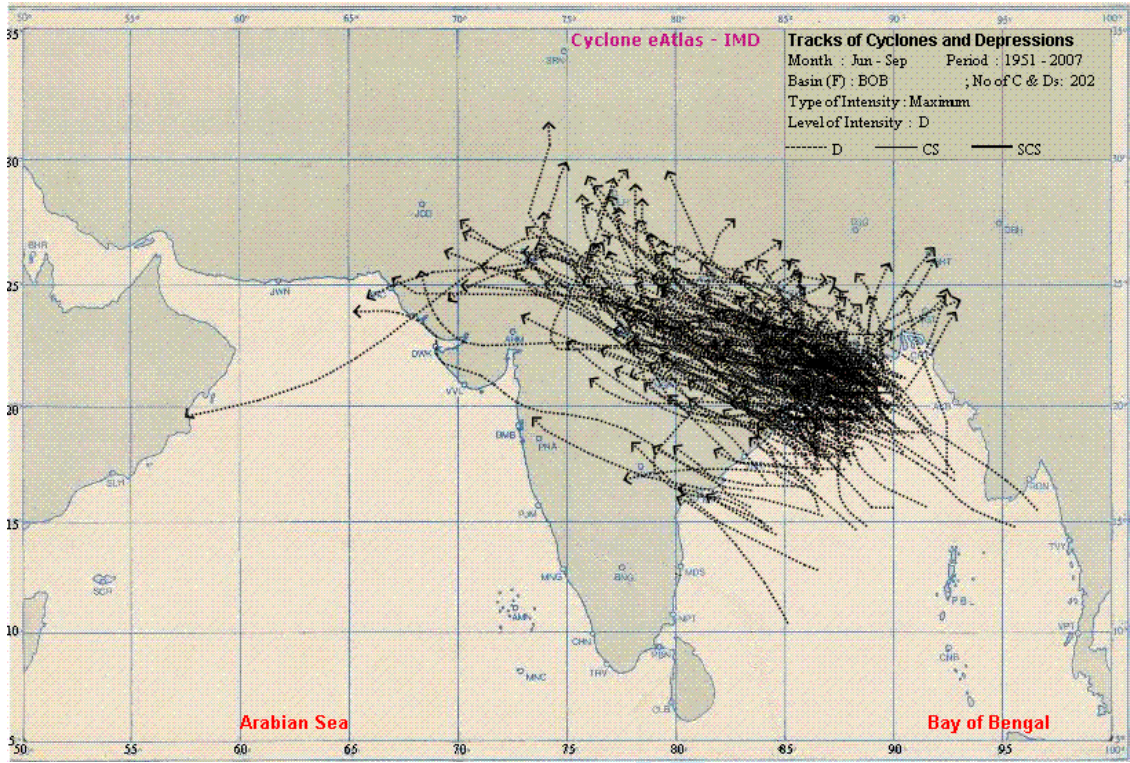


Fig. 1. Tracks of all the monsoon depressions originating from the Bay of Bengal during monsoon season (1951-2004)

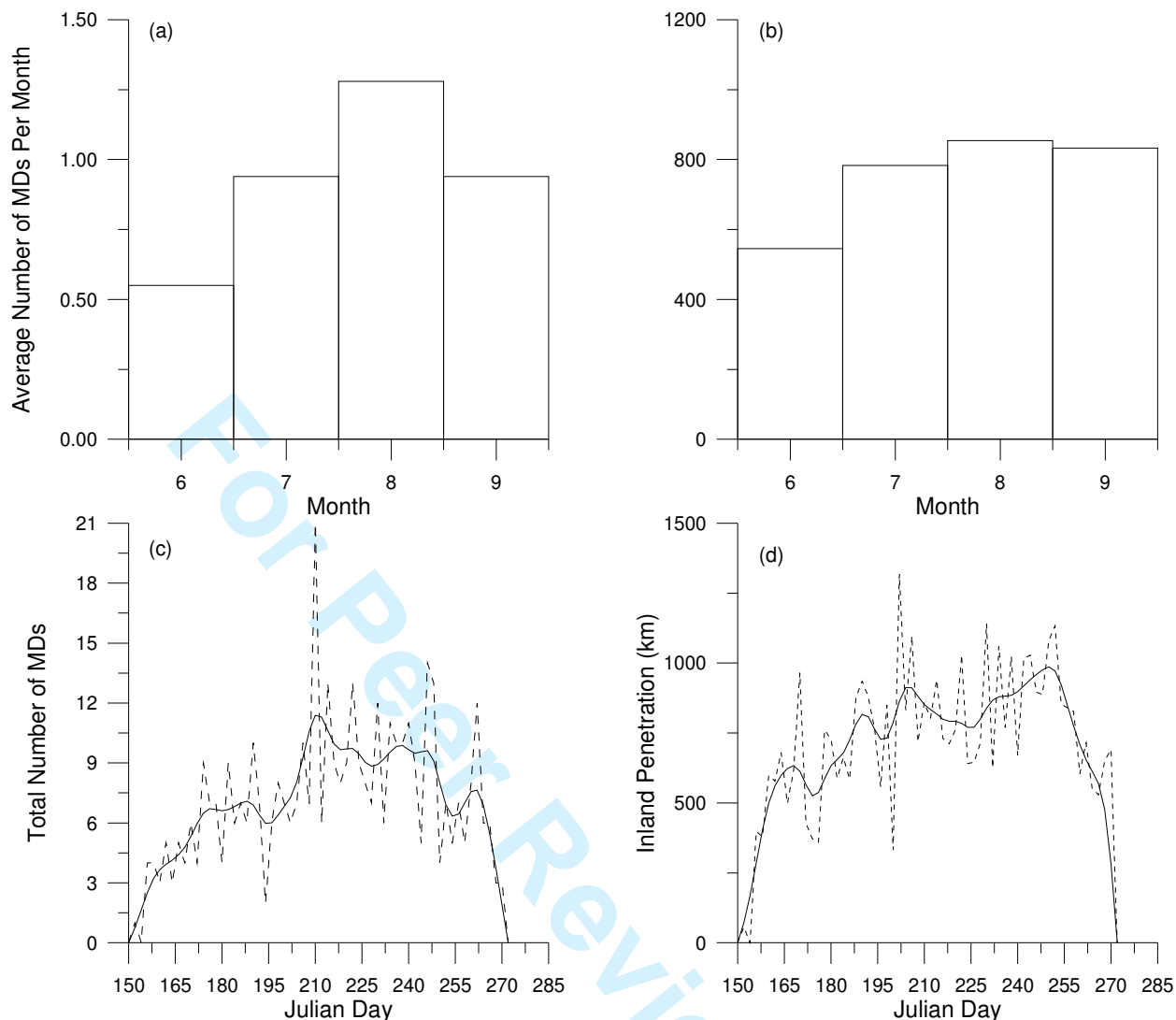


Fig. 2 .Intraseasonal variation of MDs(a) Average monthly occurrences of MDs (b) Average monthly inland penetration by MDs (c) total number of MDs formed on each day monsoon season during the period 1891-2007 (dashed line shows unfiltered values, solid line shows smoothed values) (d) same as Fig. 4-c, but for the mean inland penetration (Km) by MDs..

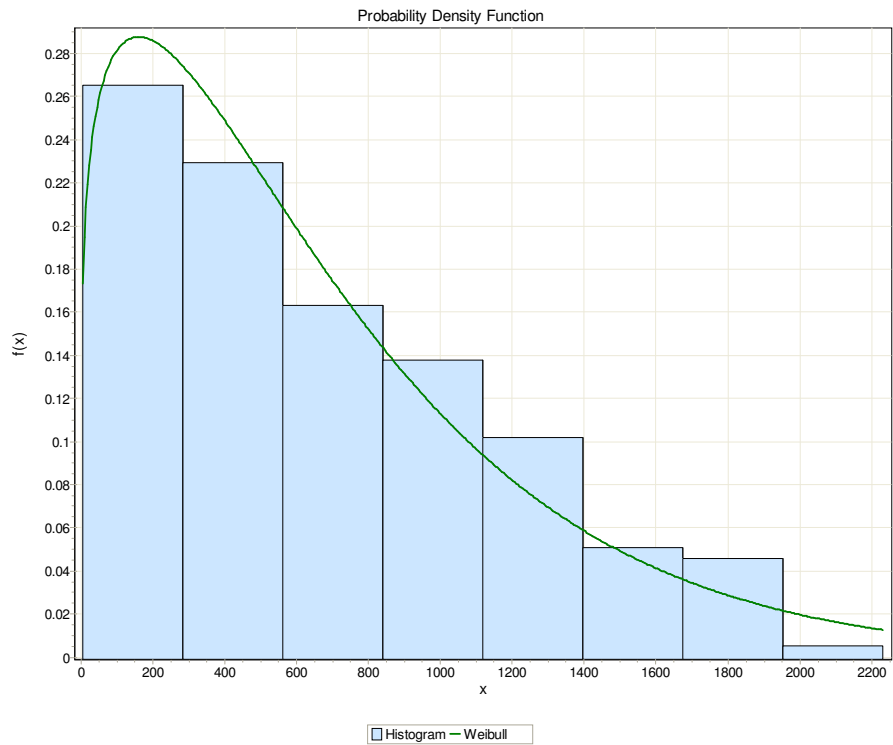


Fig. 3 . PDF of inland penetration length by MDs and the fitted Weibull distribution

Review

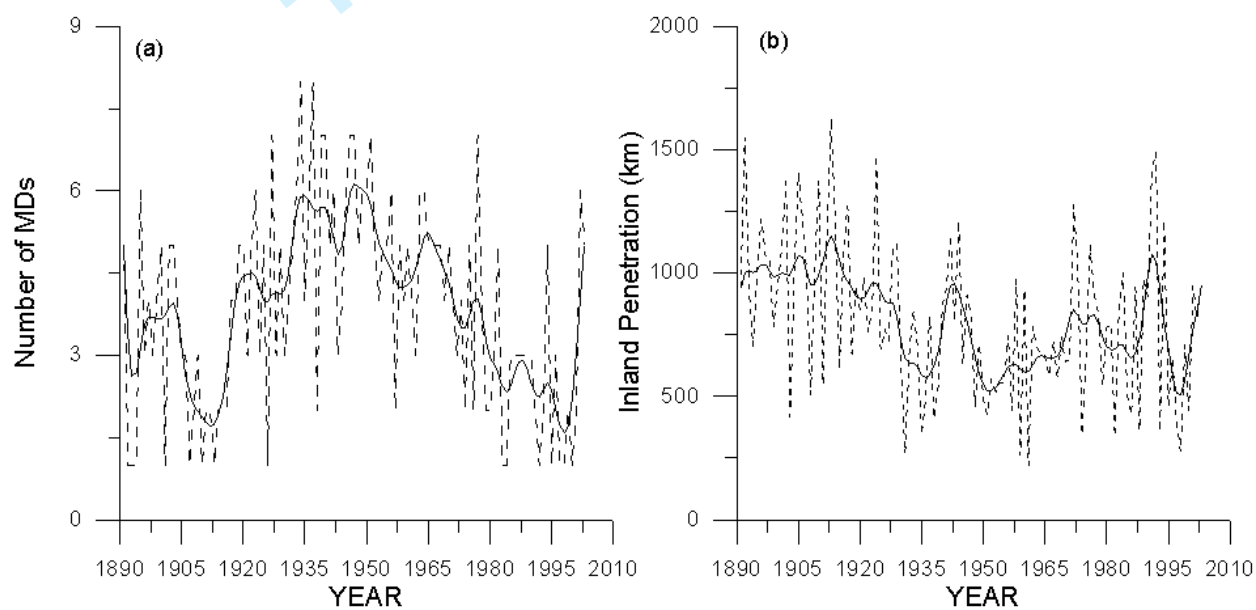


Fig.4 (a) Long-term variation of number of MDs per year (1891-2007) and (b) mean penetration length by MDs (Km). (Dashed lines show unfiltered values while solid lines show smoothed values.)

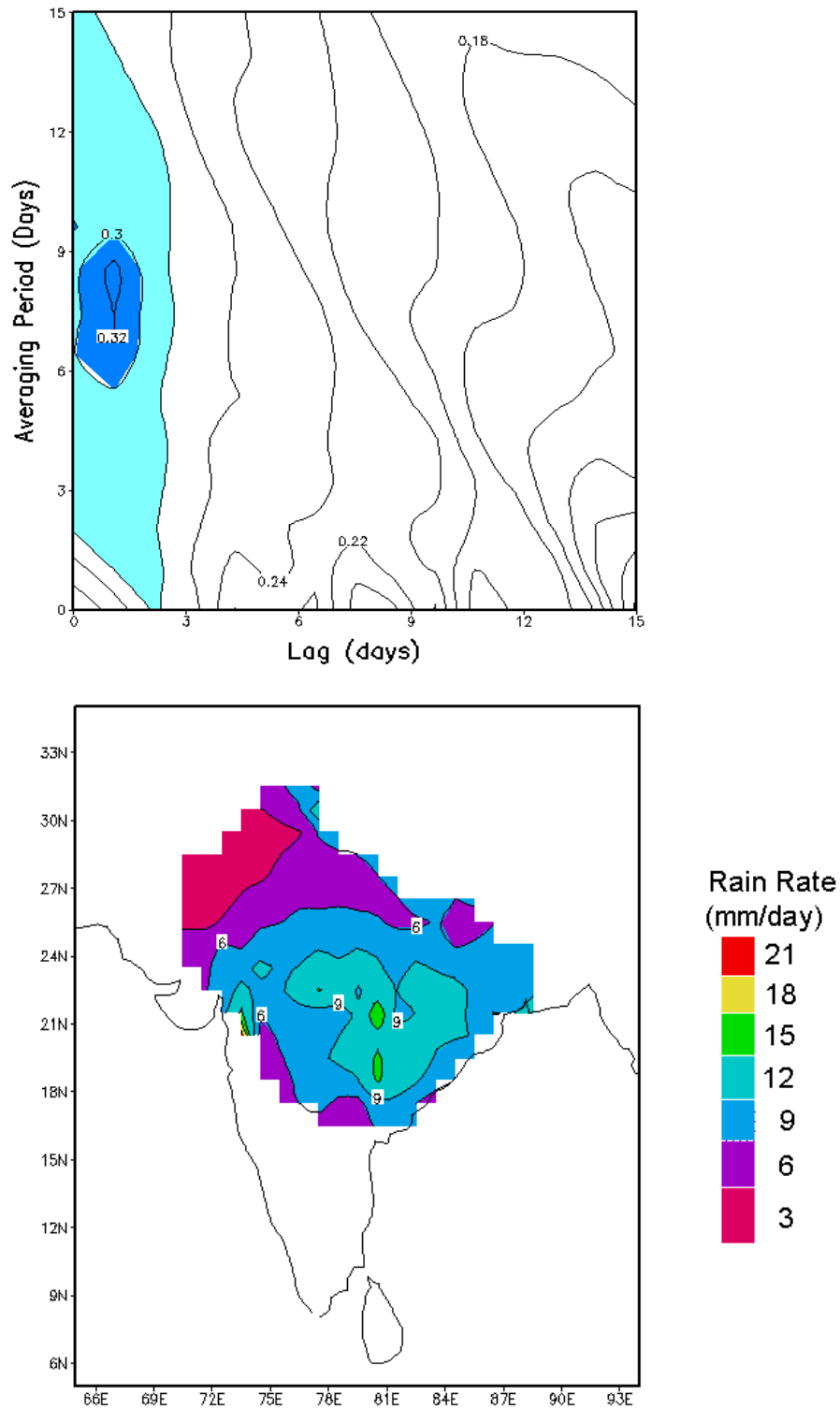


Fig. 5. (a) Correlation of IPL with pre-storm rain over the MD-Corridor (the area shown in Fig. 5-b) for various lags and averaging periods (b) mean pre-storm rainfall (for lag = 1 day and averaging period = 7 days) for all 183 cases.

1
2
3
4
5
6
7
8
9
10
11
12
13
14
15
16
17
18
19
20
21
22
23
24
25
26
27
28
29
30
31
32
33
34
35
36
37
38
39
40
41
42
43
44
45
46
47
48
49
50
51
52
53
54
55
56
57
58
59
60

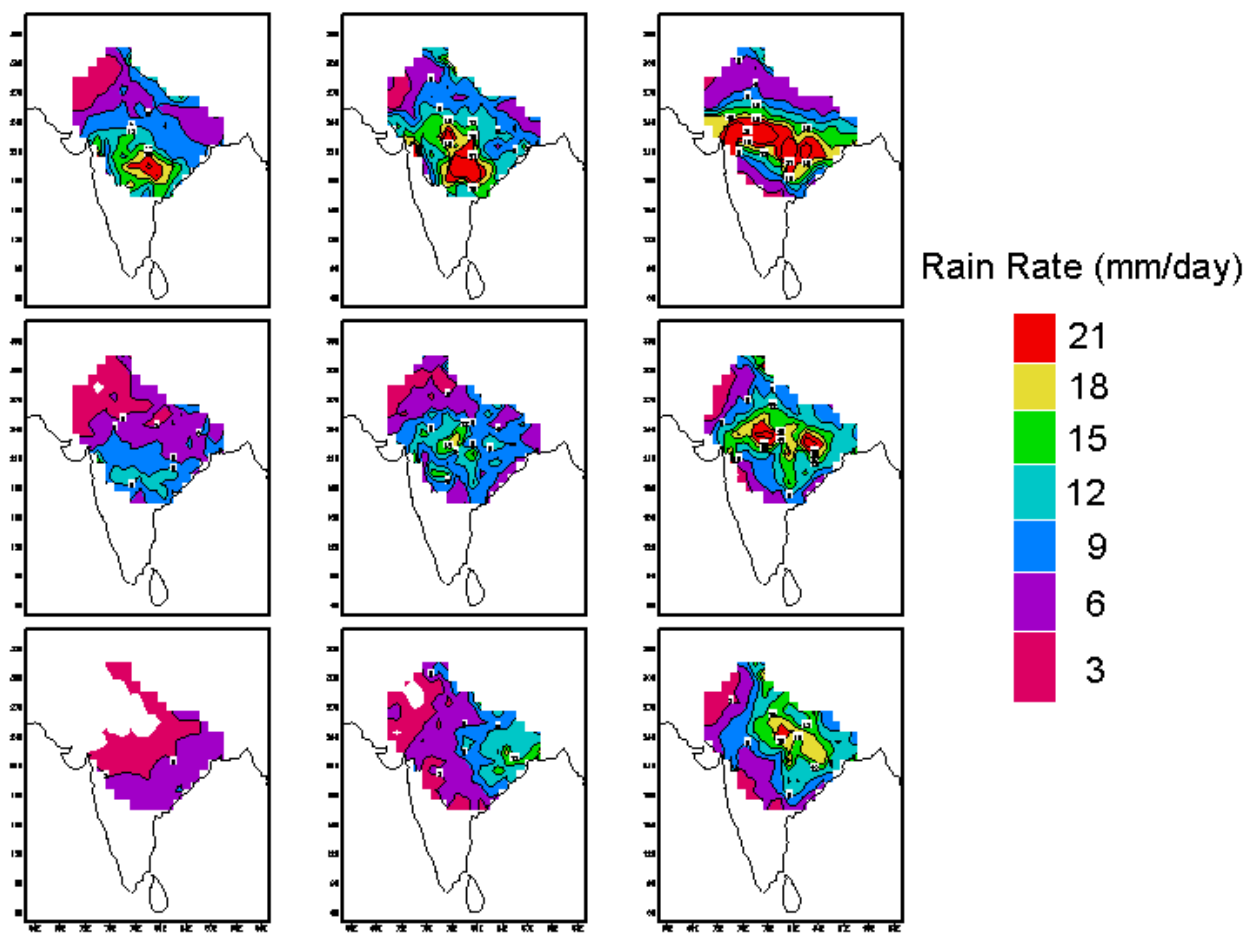


Fig. 6 . Patterns of pre-storm rainfall over monsoon trough region projected on SOM nodes.
(The order of different nodes in this figure is as indicated in Table-1.)

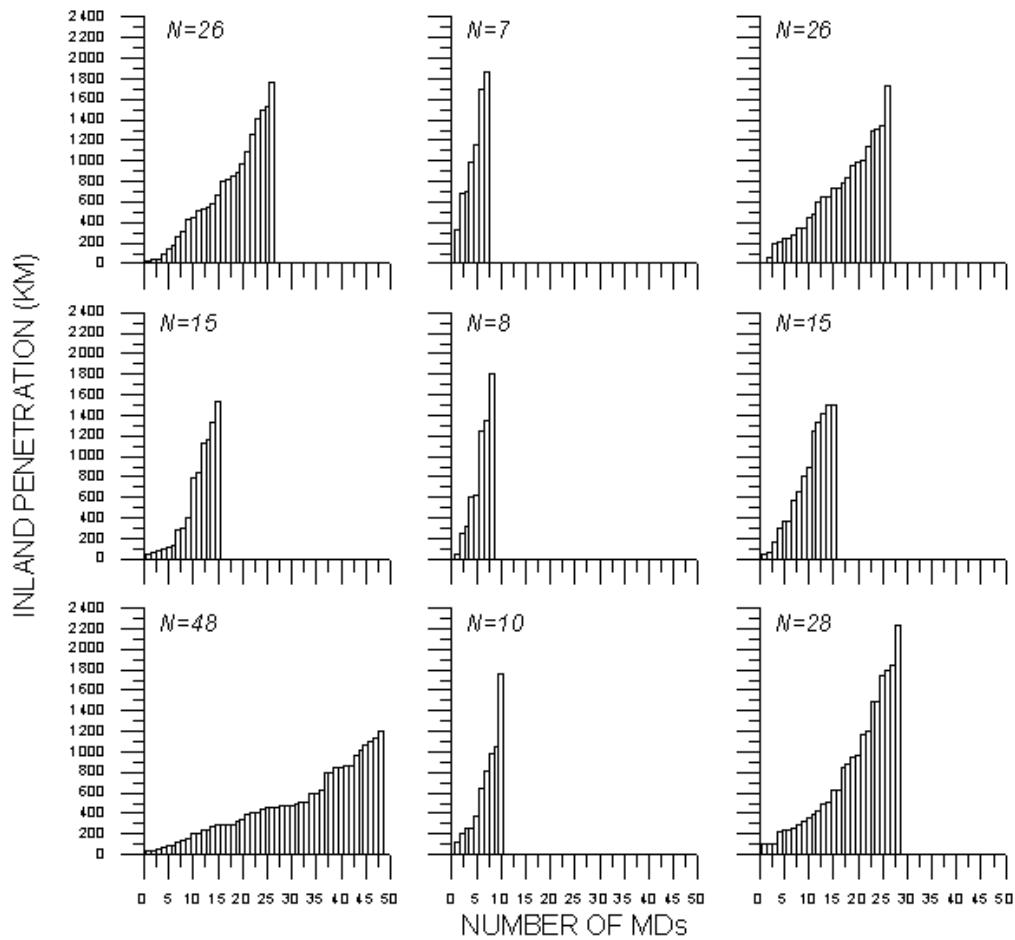


Fig. 7. Inland penetration lengths by MDs for different SOM nodes.

Each vertical bar denotes one MD event while the length of the bar represents the inland penetration. (The order of different nodes in this figure is as indicated in Table-1.)

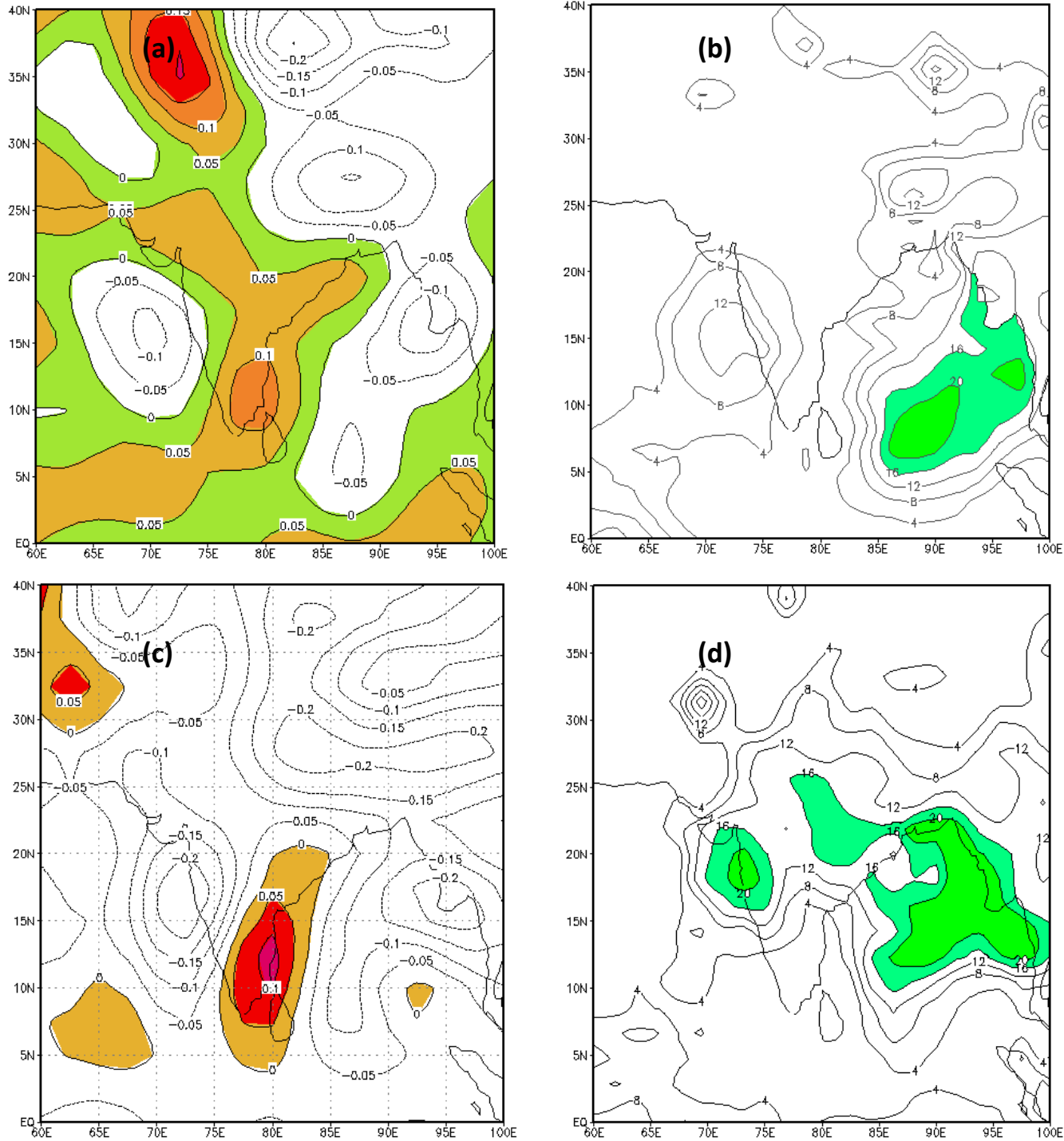


Fig. 8 . Sample figure showing the 7-day average patterns of (a) vertical velocity (ω) and (b) rainfall before the formation of an MD [formation date : 05-Aug-1972] during dry phase (SOM node [1,3]). (c), and (d) show the same parameters as (a) and (b) respectively, but for an MD during the wet node [3,1]. The later MD formed on 04-Aug-1997.

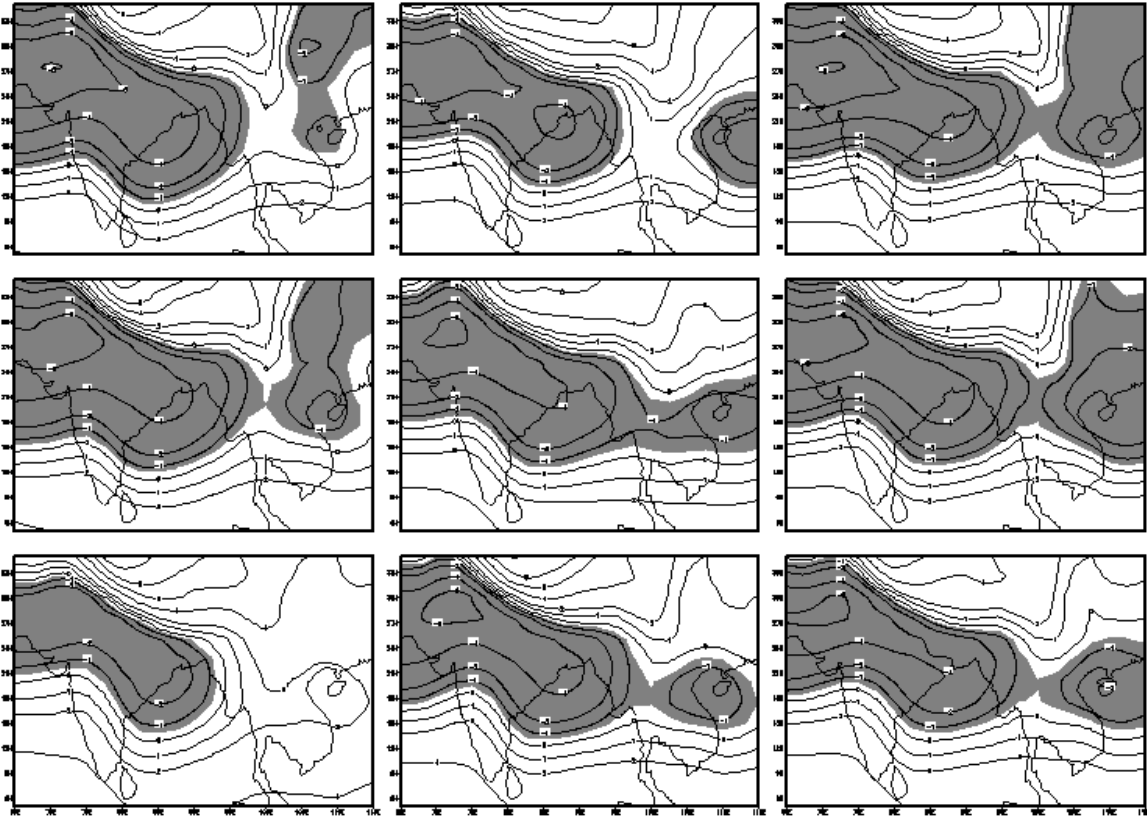


Fig. 9 .Average patterns of pre-storm sea level pressure (SLP-minus 1000 hPa) for MDs projected on different SOM nodes. The index of each node as shown in Table-1. The negative values are shaded. SLP fields denote the situation 2 days prior to the formation of MDs.

1
2
3
4
5
6
7
8
9
10
11
12
13
14
15
16
17
18
19
20
21
22
23
24
25
26
27
28
29
30
31
32
33
34
35
36
37
38
39
40
41
42
43
44
45
46
47
48
49
50
51
52
53
54
55
56
57
58
59
60

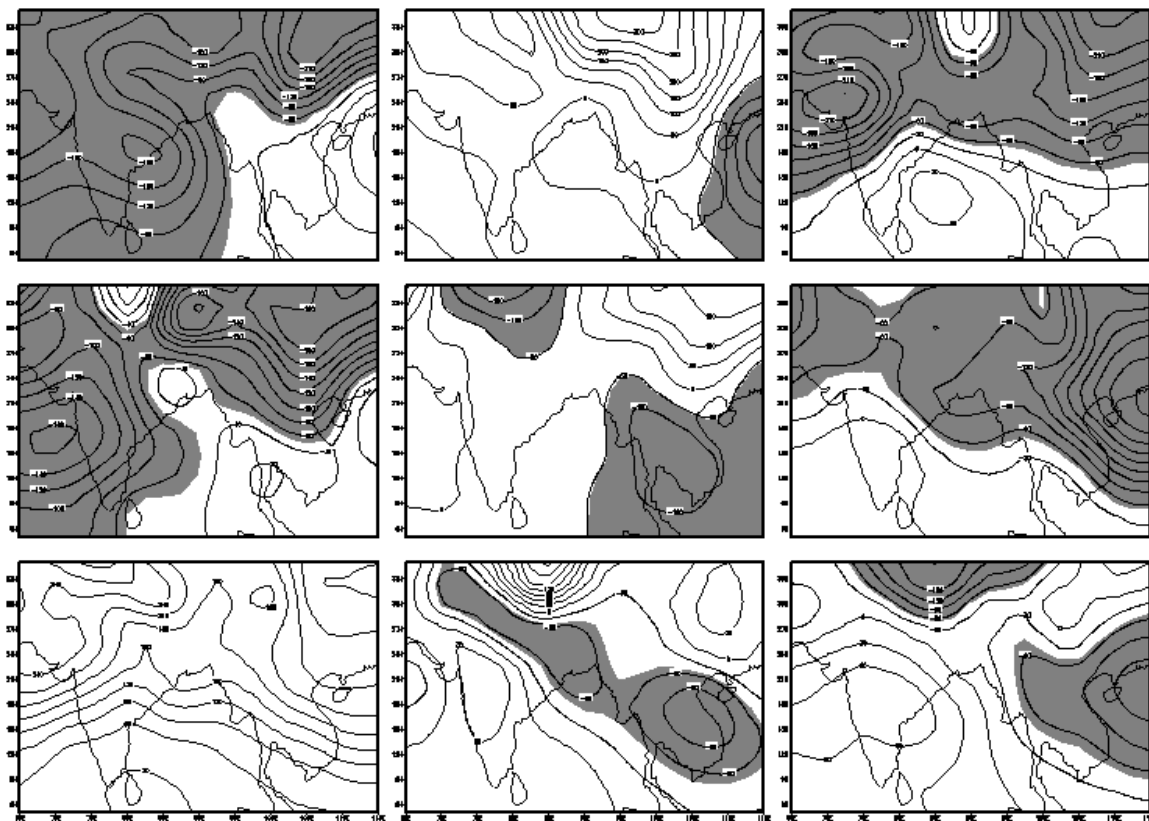


Fig. 10. Same as Fig. 9 but for SLP anomalies (unit=Pascal). Anomalies are computed with respect to the average pre-storm SLP for all 183 MDs.